NMR imaging: image recovery under magnetic fields with large non-uniformities

1978 J. Phys. E: Sci. Instrum. 11 217

(http://iopscience.iop.org/0022-3735/11/3/012)

J. Phys. E: Sci. Instrum., Vol. 11, 1978. Printed in Great Britain

NMR imaging: image recovery under magnetic fields with large non-uniformities

J M S Hutchison, R J Sutherland and J R Mallard
Department of Medical Physics, University of Aberdeen, Foresterhill, Aberdeen AB9 2ZD, UK

Received 28 June 1977, in final form 26 September 1977

Abstract In the field of NMR imaging using selective excitation techniques, a procedure is described whereby image information can be recovered with acceptable fidelity in the presence of large magnetic field non-uniformities. It entails only the running of a reference uniform sample under the same conditions as the unknown and performing a kind of deconvolution of signals. By this means, a number of different kinds of distortion can be compensated, without requiring any detailed knowledge of the particular magnetic field non-uniformity involved.

1 Introduction

One of the biggest problems of extending imaging by NMR to larger samples is that of obtaining a sufficiently uniform magnetic field over the sample volume. For a system to image portions of the human trunk, for example, this means regions with a diameter of 0·5 m or so. This can be compared with the 5 mm diameter sample region of, say, a high-resolution spectrometer, which may have a magnet weighing several tonnes. It is clearly out of the question simply to scale up all dimensions by a factor of 100.

To scale realistically, a number of things must be sacrificed. Firstly, the magnetic field and hence Larmor frequency can be dropped substantially – in proton imaging, usually to 10 MHz or less. This is normally accompanied by a loss in sensitivity in proportion to (frequency)$^{3/2}$, but is largely counteracted by the increased number of spins in the sample.

The second major sacrifice must be homogeneity of the magnetic field. Figures like 1 part in 10^7, typical of high-resolution systems, are certainly not necessary. However, the degree of uniformity required depends on the particular imaging method chosen. Perhaps the most restrictive are the 'reconstruction from projections' method (Lauterbur 1973, Hutchison *et al* 1974) and Ernst's multidimensional Fourier transform method (Kumar *et al* 1975). Much less restrictive are the sensitive point method of Hinshaw (1974) and the various procedures under the general description of 'selective excitation' (e.g. Mansfield and Maudsley 1976). It is our particular variant of this last method which is the subject of this paper.

With both the 'projections' method and Ernst's method, the magnetic field over the whole sample must be uniform to within the equivalent of one picture element or 'pixel'. For example, if the applied field gradient induces a splitting of 10 kHz across the whole sample, and the sample image width is 100 pixels, then each pixel is 100 Hz wide and the necessary field uniformity is the equivalent of this, or $2{\cdot}4 \times 10^{-6}$ T for protons. For a Larmor frequency of 10 MHz, this represents 1 part in 10^5. Expressed in another way, the original field must be uniform to within 1% of the maximum field difference introduced by the applied field gradient. In either of the methods mentioned above, information is irretrievably lost if the non-uniformity exceeds this small percentage, which we shall call the field distortion factor (see below).

The particular treatment of selective excitation which we propose can tolerate field distortion factors of up to about 50% without irretrievable loss of information.

2 The pulse sequence

The sequence used and assumed in all the simulations in this paper is shown in figure 1. It is a subset of the full sequence

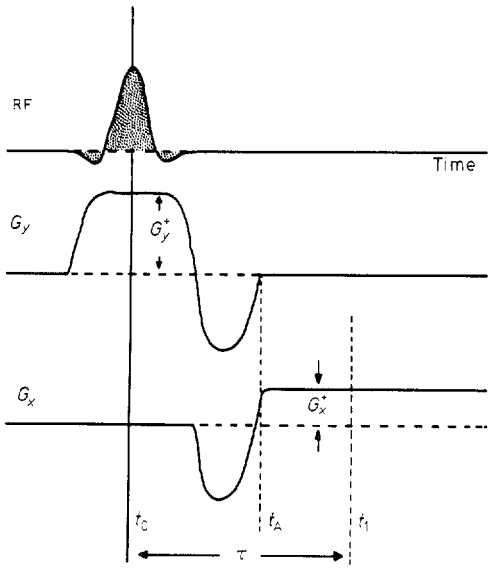

Figure 1 The pulse sequence used for two-dimensional imaging. RF is the modulating function for the radio frequency magnetic field. G_y and G_x are the magnetic field gradient waveforms. The observation period begins at t_A.

discussed by us elsewhere (Sutherland and Hutchison 1978) in that operations are restricted to the x–y plane; sample thickness in the z direction is assumed to be sufficiently small that all spin packets having common x and y coordinates behave identically. This is a basic selective excitation sequence. A spectrally tailored 90° RF pulse is applied together with a gradient G_y to excite spins in a narrow strip lying close to $y=0$. Then follows a negative portion of G_y, whose function is to *rephase* the spins across the selected strip. Simultaneously, G_x is driven negative to *dephase* the spins along the strip. G_x is then driven to a constant positive value, and the observation period begins at t_A. In the ideal case, all the spins come back into phase at t_1, a time τ after the centre of the RF pulse. This is a form of spin echo, but should not be confused with the usual type induced by a 180° pulse. The in-phase condition is met when

$$\int_{t_0}^{t_1} G_x \, dt = 0 \quad \text{and} \quad \int_{t_0}^{t_1} G_y \, dt = 0. \tag{1}$$

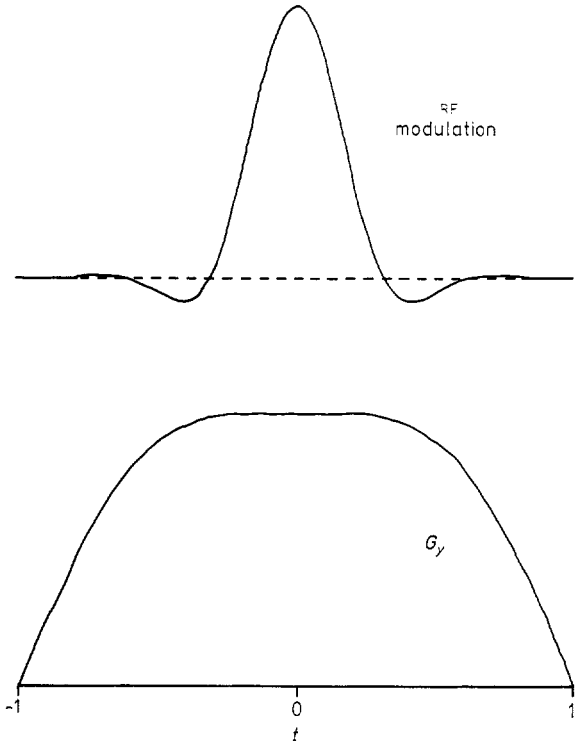

Figure 2 Details of the RF modulation and y gradient. RF modulation = sinc $(3{\cdot}2\,t)$ exp $(-5\,t^2)$.
$G_y = (\cos 1{\cdot}57\,t - 0{\cdot}12 \cos 4{\cdot}71\,t)/0{\cdot}88$. t is normalised time relative to t_0 as origin.

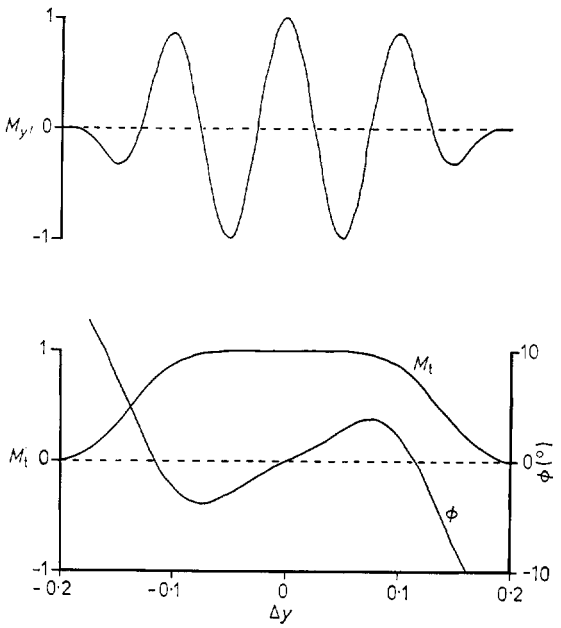

Figure 3 Spin magnetisation as a function of normalised distance from the centre line of the selected strip, Δy. This simulation uses the RF and gradient waveforms of figure 2, and Δy is normalised by setting $\gamma = 1$. Upper curve: $M_{y'}$ is the component of magnetisation along y' in the standard rotating coordinate frame, in the case of no rephasing. Lower curves: M_t is the transverse magnetisation and ϕ the phase, in the case of optimum rephase.

The actual shapes of the G_x and G_y waveforms are unimportant, provided that the following conditions are met:
(i) during the RF pulse, $G_x = 0$ and $G_y = G_y^+ = \text{constant}$;
(ii) during the observation period, $G_y = 0$ and $G_x^+ = \text{constant}$.
Otherwise signal processing becomes extremely complicated.

There is no need to have sharp-edged rectangular gradient drive waveforms, which is very useful in practice since the field gradient windings present an inductive load.

Figure 2 shows the shape of the gradient drive G_y, and the RF modulation is an apodised sinc function to give a roughly rectangular spectral profile. The gradient drive waveform is composed of fundamental and third-harmonic sine waves, and has been implemented quite successfully on the scale required using thyristor switching and resonant LC circuits (see appendix).

Figure 3 shows the spin magnetisation across the selected strip, firstly with no rephasing and then with optimum rephasing. $M_{y'}$ is the magnetisation in the rotating coordinate frame defined by the natural Larmor precession of spins located at $x = y = 0$ (in the absence of RF or gradient fields, the spin magnetisation maintains a fixed orientation in the rotating frame). The directions of y and y' coincide at time t_0. M_t is the amplitude of the transverse magnetisation and ϕ its angle relative to the y' direction. That is,

$$M_{y'} = M_t \cos\phi; \quad M_{x'} = M_t \sin\phi. \tag{2}$$

In practice, ϕ is also the phase of the nuclear induction signal. Since the signal from any region of the selected strip is proportional to the vector integral of transverse magnetisation across the strip, it is in our interests to have as little phase variation as possible across the strip – hence the desirability of the rephasing addition to the G_y waveform. The phase is within $\pm 5°$ over most of the strip width, which is quite acceptable.

To select a different strip, the carrier frequency of the RF pulse is shifted by an amount Δf. In practice, this must be done using phase-lock techniques so that the phase of the carrier as measured at the centre of the RF pulse (time t_0) remains unchanged. This procedure selects a new strip, parallel to the original, at

$$y = \frac{\Delta f}{\gamma G_y^+} \tag{3}$$

where γ is the gyromagnetic ratio of the spins, and G_y^+ is the value of G_y during the RF pulse. Since G_y^+ is not perfectly constant, both in expected practice and in the simulation, a certain degradation in the strip selection should occur as Δf is increased. Analysis shows, however, that the result is still acceptable after moving the strip through 20 times its width.

3 Effects of field non-uniformity on the signal

Let us suppose that the magnetic field applied to the sample consists of a uniform part H_0 and an error field $E(x, y)$ which are not time-dependent. Taking into account the time-dependent gradient fields, we obtain the full expression for the field seen by a spin packet at (x, y) at time t:

$$H_z = H_0 + E(x, y) + xG_x(t) + yG_y(t). \tag{4}$$

It is easily shown that any given spin packet now experiences an additional phase error $\Delta\phi_E$ which depends only on the inhomogeneity E and the time t after the centre of the RF pulse:

$$\Delta\phi_E = 2\pi\gamma t E. \tag{5}$$

We now consider the signal originating from a short section of the selected strip. During the observation period

(when G_x^+ is present) and in the absence of the error field E, the phase of the spin precession, relative to the y' direction, will be

$$\phi = 2\pi\gamma x G_x^+ (t-\tau) \tag{6}$$

where $\tau = t_1 - t_0$, the time of the spin-echo centre. In the presence of E, the total phase shift ϕ_T will be the sum of (5) and (6):

$$\phi_T = \phi + \Delta\phi_E = 2\pi\gamma[xG_x^+(t-\tau) + tE]. \tag{7}$$

If, now, the short section is considered to be non-infinitesimal in extent, then it can be considered as giving rise to a *group* spin echo, whose centre occurs when all the spins are most nearly in phase with each other, i.e.

$$\frac{\partial\phi_T}{\partial x} = 0. \tag{8}$$

Applying this criterion to equation (7) yields an expression for the time of the group spin echo:

$$t_{echo} = \frac{\tau G_x^+}{G_x^- + \partial E/\partial x}. \tag{9}$$

Equation (9) may now be rearranged to give the time displacement $\Delta\tau$ of the group spin echo due to the error field E:

$$\Delta\tau = t_{echo} - \tau = -\tau\left(\frac{\partial E/\partial x}{G_x^+ + \partial E/\partial x}\right). \tag{10}$$

The importance of this expression lies in information theory, which tells us that the group spin-echo centre must lie within the observation period, otherwise information concerning the group is irretrievably lost. This places a lower bound on $\Delta\tau$, namely

$$\Delta\tau > t_1 - t_A. \tag{11}$$

Since the observation period can be extended indefinitely, there is no well defined upper bound on $\Delta\tau$; spin–spin relaxation processes will cause a gradual deterioration as $\Delta\tau$ is increased. Field foldback occurs when $\partial E/\partial x = -G_x^+$, the condition when $\Delta\tau = \infty$, and the position along the strip is no longer uniquely determined by H_z, again signifying loss of information.

In the presence of an indeterminate error field E, with its concomitant phasing errors, the simple Fourier transform of the nuclear induction signal no longer represents the line profile, since it requires the existence of a reference time when all the spins are in phase. However, information theory also tells us that, as long as the above constraints on $\Delta\tau$ are met, the line profile can be recovered completely. The method is described in §5.

4 Effects of field non-uniformity on the selection process

The locus of the selected strip is given in general by

$$\Delta f/\gamma = E(x, y) + yG_y^+ \tag{12}$$

which reduces to equation (3) in the absence of an error field. It is perhaps more instructive at this point to consider a particular type of error field consisting only of second-order terms:

$$E = k(x^2 + y^2). \tag{13}$$

This is a circular pattern of the kind that might be expected in an air-cored magnet based on circular coils.

We can now define a field distortion factor D, briefly referred to in §1, as

$$D = \left|\frac{2kr_{max}}{G}\right| \tag{14}$$

where G is the applied gradient at the time in question, and r_{max} is the maximum radius of the sample. $D = 1$ represents the limiting case of field foldback at the edge of the sample. In particular, during the observation period

$$D = \left|\frac{\partial E/\partial x}{G_x^+}\right|_{x=x_{max}}. \tag{15}$$

Figure 4 shows the locus of the selected strip and the field contours during (*a*) excitation and (*b*) observation, for

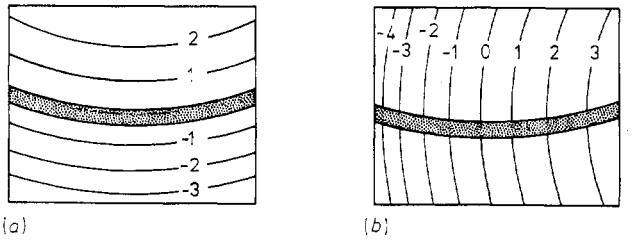

Figure 4 Field contour lines and the locus of the selected strip during (*a*) excitation and (*b*) observation, when field distortion of the form given by equation (13) is present.

$\Delta f = 0$. The curvature of the selected strip is proportional to D_y, the distortion factor during excitation being, in this case, approximately 0·3. Two further effects occur when Δf is altered to obtain different image lines.

(1) The width of the selected strip is proportional to the spacing of the contour lines, which alters across the sample. Hence, signal sensitivity will vary according to the line chosen.

(2) The line spacing and curvature alter across the sample, giving rise to geometrical distortion of the image.

From figure 4(*b*) it can be seen that there is a bunching of contour lines towards one end of the strip, which will manifest itself as a location error of features on the line profile, i.e. another geometrical distortion. The effect is proportional to D_x, equal to 0·3 in this diagram. The full geometrical distortion can be represented by a grid formed by superimposing the field contour lines from figures 4(*a*) and (*b*). It should, however, be noted at this stage that in any practical system G_y^+ will generally be many times larger than G_x^+, thus reducing D_y substantially. Figure 4(*a*) is thus rather exaggerated, and one would expect the selected strips to be much straighter and more evenly spaced.

5 Recovery of the line profile

There are two stages in this process. The first stage corrects the phase error. Contrary to expectation, this does not require a detailed knowledge of the error field E. The procedure is to run the system with a reference sample, which is simply a uniform distribution of spins, and obtain the reference spin-echo waveform $r(t)$. In practice this entails filling the sample region with water (for proton imaging), preferably doped to bring its spin–spin relaxation time T_2 to a value similar to that of the unknown sample. The unknown sample is then run with identical settings to obtain its spin-echo waveform $s(t)$. The waveforms s and r are undefined for $t < t_A$ and must be assumed to be zero. The Fourier transforms $S(\omega)$ and $R(\omega)$ are then obtained and an intermediate function is computed:

$$F(\omega) = S(\omega)/R(\omega). \tag{16}$$

The function F has now been corrected in phase and

amplitude with respect to the reference. The reverse transform $f(t)$ is effectively $s(t)$ deconvoluted by $r(t)$. However, the sidebands of F in t space are less than ideal, being asymmetrical; furthermore, this asymmetry is ω-dependent. The simplest way to correct this is to deal with the function $f(t)$. $f(t)$ represents the sidebands of F and has a 'before' sideband ($t<0$) and an 'after' sideband ($t>0$). Ideally these should be matched, but they are not, and it is the 'before' sideband which suffers most from the effects of phase errors. The solution is simply to remove this sideband according to the following scheme. Let

$$\begin{aligned} h(t)&=f(t), && t>0 \\ h(0)&=\tfrac{1}{2}f(0) \\ h(t)&=0, && t<0. \end{aligned} \tag{17}$$

Then let $H(\omega)$ be the Fourier transform of $h(t)$.

The real part of $H(\omega)$ is taken as the line profile. The imaginary part is its Hilbert transform which is of no interest since it contains no extra information. The assignment $h(0)=\frac{1}{2}f(0)$ is largely irrelevant when the ordinates t and ω are continuous, but it becomes important in computer processing, where they are stepped in discrete intervals. Without this assignment, the DC level of the final line profile is incorrect.

6 Simulated examples

Figure 5 shows the effect of the procedure on a simulated sample consisting of three rectangular pockets of spins,

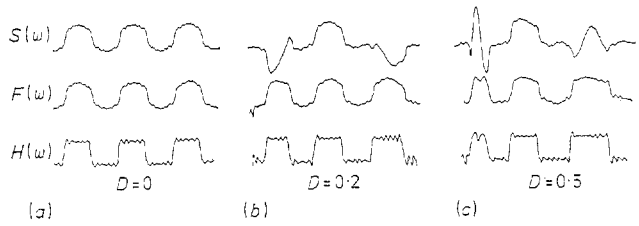

Figure 5 Computer simulation waveforms for the functions S, R and H for a sample of three rectangular pockets of spins. Results are shown for three different field distortion factors: (*a*) $D=0$, (*b*) $D=0{\cdot}2$ and (*c*) $D=0{\cdot}5$.

subject to the field non-uniformity described by equation (13). In all cases the observation period extends from $t_1-\frac{1}{2}\tau$ to $t_1+2\tau$. The phase error $\Delta\phi_E$ is proportional to D and amounts to approximately 10 rad at the edges of the sample for $D=0{\cdot}5$.

It is easily seen that the function $H(\omega)$ is a closer representation of the original spin distribution than F, even when there is no field distortion. Note also the bunching of detail towards the left-hand side of the line profile; this is a consequence of the geometrical distortion of the field contour lines illustrated in figure 4(*b*). We note that, although the amplitude of S is affected by this bunching process, those of F and H are not, being compensated by a similar effect on $R(\omega)$. Technically, it should be possible to 'unbunch' $H(\omega)$ using the phase information present in $R(\omega)$, but this would still leave geometrical distortion due to the curvature of the contour lines in figure 4(*b*) and curvature of the selected line (figure 4(*a*)). These various geometry corrections are not within the scope of this paper.

There is a certain amount of ringing evident on the $H(\omega)$ waveform. In part this is due to the sharp cut-off of $s(t)$ and $r(t)$ in the time domain, and a certain amount of apodisation of these functions would probably help. However, another factor is the out-of-band behaviour: the reference sample is necessarily of finite extent, so that for values of ω outside the normal range, $R(\omega)$ will approach zero. Since $S(\omega)$ is divided by this to form $F(\omega)$, the latter becomes the ratio of two small quantities, thus giving rise to large spurious values. This would especially affect the real situation where noise is present. The spurious values of F only occur in out-of-band regions and so do not appear on the F waveform, but they generate ripples on the H waveform which extend back into the viewed region. By incorporating a conditional procedure of the form

$$F(\omega)=0 \qquad \text{if } |R(\omega)|<\epsilon \tag{18}$$

and choosing ϵ appropriately, these effects can be reduced. This kind of problem is inherent in any deconvolution process. In the simulated examples, ϵ was set to 1% of the midband amplitude of R, mainly to avoid the disaster of division by zero, but a higher value of ϵ might prove more useful.

7 Conclusions

A procedure has been found whereby image information can be recovered with acceptable fidelity in the presence of large magnetic field non-uniformities. It is operable at a field distortion level ($D=0{\cdot}5$) which is at least an order of magnitude worse than that at which reconstruction from projections breaks down. Although geometrical distortions are introduced, the signal level ($H(\omega)$) corresponds to the spin density in the appropriate region. It requires only that a reference uniform sample be run under the same conditions as the unknown.

The procedure will also compensate for spatial variations in sensitivity due to non-uniformity of the RF magnetic field. However, in practice, a number of effects may degrade its performance. Probably the most severe of these are phase shifts due to eddy-current induction within the sample. To get ideal performance, this would require that the dielectric properties and geometry of sample and reference be identical, which is obviously impossible to achieve, but some sort of approximate match may be usable in practice.

Since the transverse magnetisation of a spin packet decays with a time constant T_2, differences in T_2 between different regions of the sample, or between sample and reference, will alter the performance. The effects are unlikely to be too severe provided that τ is substantially less than T_2.

The effects of non-uniformity of the gradient fields have not been considered in this paper. We believe that, to a first order, the only effect is a location error, but this remains to be investigated.

The procedure as described has been two-dimensional, i.e. confined to the x–y plane. In the three-dimensional case, with non-uniformity in z, this plane would become a curved surface. If additional selection is carried out in z, this curved surface is the one selected, and not only does it have a finite selection thickness Δz, but also Δz will vary as a function of x and y, giving rise to variations in spin sensitivity. Once again, these variations are compensated by our procedure.

The magnetic field non-uniformity function E must be the same for reference and unknown. In practice, this would mean that large ferromagnetic objects in the vicinity such as filing cabinets and oscilloscopes, *must not be moved* between running the reference and running the sample. E also includes any long-term drift of the main field, so that field stability remains as important as before.

Acknowledgments
The authors wish to acknowledge the help and support of the University of Aberdeen Computing Centre, without whom this work would not be possible.

Appendix Production of the y field gradient waveform, G_y
The circuit used is shown in figure 6. The current in the

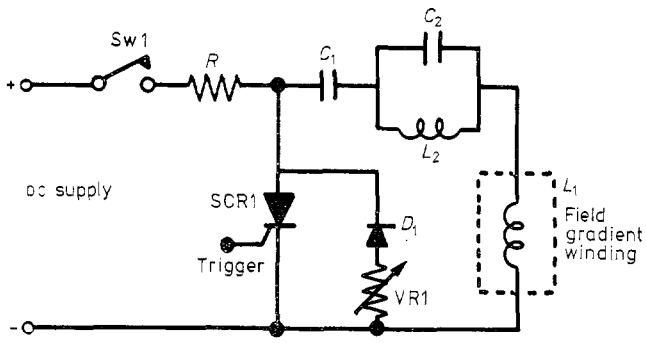

Figure 6 The electrical circuit used to generate the G_y gradient waveform.

gradient windings L_1 is

$$I(t)=I_0(\sin \omega t+k \sin 3\omega t) \tag{A.1}$$

where t is measured from the instant of firing SCR1. On the assumption that L_1 is fixed, the design formulae are

$$C_1=\frac{3+k}{(3+9k)\,\omega^2 L_1} \tag{A.2}$$

$$\frac{1}{C_2}=10\,\omega^2 L_1-9\,\omega^4 C_1 L_1^2-\frac{1}{C_1} \tag{A.3}$$

$$\frac{1}{L_2}=9\,\omega^4 C_1 C_2 L_1. \tag{A.4}$$

The condition for a maximally flat top is $k=\frac{1}{9}$. In practice it is better to make k slightly greater (0·12–0·14). There is also a droop caused by resistance in L_1 and L_2, which can be compensated by lowering C_2. Values used in practice were: $L_1=10$ mH, $L_2=2{\cdot}7$ mH, $C_1=64$ μF, and $C_2=40$ μF, giving a half-cycle of approximately 2·8 ms. VR1 is used to adjust the amplitude of the rebound half-cycle which occurs naturally when D_1 is incorporated. This rebound half-cycle now constitutes the rephase gradient pulse, with the added bonus that C_1 is left partially charged in preparation for the next sequence. Sw1 is left open until the observation period has passed, then it is closed to charge C_1 fully through R. This delay is necessary to satisfy $G_y=0$ during observation, since the charging current flows in L_1.

References

Hinshaw W S 1974 *Phys. Lett.* A **48** 87–8

Hutchison J M S, Goll C C and Mallard J R 1974 *Proc. 18th Ampere Congr., Nottingham* eds P S Allen, E R Andrew and C A Bates (Nottingham: University) pp 283–4

Kumar A, Welti D and Ernst R R 1975 *J. Magn. Res.* **18** 69–83

Lauterbur P C 1973 *Nature* **242** 190–1

Mansfield P and Maudsley A A 1976 *Phys. Med. Biol.* 847–52

Sutherland R and Hutchison J M S 1978 *J. Phys. E: Sci. Instrum.* **11** 79–83